Supplementary Information

Genetically encoding a light switch in an ionotropic glutamate receptor reveals subunit-specific interfaces

Shujia Zhu[&], Morgane Riou[&], C. Andrea Yao, Stéphanie Carvalho, Pamela C. Rodriguez, Olivier Bensaude, Pierre Paoletti* and Shixin Ye*

& equally contributing authors, * co-last authors.

Correspondence should be addressed to: pierre.paoletti@ens.fr or yelehman@biologie.ens.fr

Supplementary information includes:

SI Materials and Methods

Supplementary Figures 1−10

SI Materials and Methods

Molecular biology and plasmid construction

Plasmid pSVB.Yam carrying the gene encoding the amber suppressor tRNA derived from B. *stearothermophilus* Tyr-$tRNA_{CUA,}$ and the aminoacyl-tRNA synthetases (aaRS) construction for AzF and Bpa derived from *E. coli* TyrRS have been previously described (1, 2). The pcDNA3-based expression plasmids for rat GluN1-1a (named GluN1 herein), rat GluN2A and mouse ε2 (named GluN2B herein) subunits and sequencing procedure have been described previously (3, 4). Chimeras with exchanged NTDs, GluN2A-2B(NTD), GluN2A-2B(NTD+L), GluN2B-2A(NTD) and GluN2B-2A(NTD+L), were obtained as described in (5). The site-direct amino acid or amber stop codon mutations were introduced into GluN1 or GluN2 by using the Quikchange mutagenesis strategy (Stratagene). Chimeras with exchanged upper lobes or interfaces, Glu2A-2BUL and GluN2A-2BUL-loop were obtained by a modified protocol of the Quikchange mutagenesis. GluN2A-2BUL represents DNA fragments of GluN2A M1-S142 and Y286-P359 replaced with GluN2B M1-S141 and Y287-P360. GluN2A-2BUL-loop construct was generated based on the GluN2A-2BUL with additional DNA fragment of GluN2A-$_{205}$TFSED replaced with GluN2B-$_{208}$MSLDDGD. In GluN1-3D, the '3D' represents the residues K131, K322 and R323 mutated to aspartate (D). In GluN2B-3K, the '3K' represents the residues D206, D210 and D213 mutated to lysine (K).

The bidirectional plasmid coding for both the suppressor tRNA and the aaRS was constructed as following: the tRNA was cloned between XhoI and SphI sites in pET21d(+) providing the pET21-tRNA Stea plasmid. A MluI-BstZ17I fragment from the pCDNA3.1 AzFRS containing the AzF synthetase (1) was cloned into MluI and BstZ17I sites of pET21-tRNA Stea providing the final pET21-tRNA-AzFRS plasmid.

The GFP-Y182amb-GluN2B subunit corresponds to the wild-type GluN2B subunit with an N-terminal fused enhanced green fluorescent protein (eGFP) with an amber stop codon at position Y182 (see ref. (6)). The eGFP cDNA fragment was inserted between the 5th and 6th codons after the sequence for the signal peptide (as described in ref. (7)).

Cell culture, plasmid DNA delivery and UAA incubation

Oocytes were prepared and injected as described previously (3). Recombinant NMDARs were expressed in *Xenopus* laevis oocytes after nuclear injection of 36 nl of a mixture cDNAs encoding various GluN1 and GluN2 subunits (ratio 1:1, 10 ng/µl for GluN2A and 30 ng/µl for GluN2B). For UAA incorporation, oocytes were co-injected with a 36 nl mixture of cDNAs

containing GluN1, GluN2, Yam, and aaRS as follows, unless otherwise indicated in the text: GluN1-Y109amb (40 ng/µl), GluN2A wt (40 ng/µl), Yam (10 ng/µl), AzFRS (2 ng/µl); or, GluN1-Y109amb (60 ng/µl), GluN2B wt (60 ng/µl), Yam (10 ng/µl), and BpaRS (10 ng/µl) or AzFRS (2 ng/µl). After injection, oocytes were incubated at 19°C in a Barth solution supplemented with gentamicin sulfate (50 ng/ml) and D-APV (50 µM). AzF (Chem-Impex International) was dissolved with sonication in Barth solution (stock solution at 10 mM), and diluted (2 mM) for oocytes incubation. Bpa (Bachem) was dissolved in ddH_2O (stock solution at 200 mM) by adding equal molar of NaOH, and subsequently diluted (1 mM) in Barth solution (8).

Human embryonic kidney (HEK) cells were cultured in DMEM medium supplemented with 2 mM glutamine, 10% heat-inactivated fetal calf serum and penicillin–streptomycin (5000 U/ml). HEK cells with 20-40% confluency were transfected using the jetPRIME transfection reagent (Polyplus-Transfection). Cells were co-transfected with a DNA mixture of wild-type GluN1 or GluN1-Y109amb, GFP-Y182amb-GluN2B and the bidirectional plasmid pET21-tRNA-AzFRS (ratio of 1:1:1; 0.75 µg total DNA per coverslip). AzF (1 mM) and the competitive NMDAR antagonist D-APV (200 µM) were added to the culture medium immediately after the transfection.

Dissociated hippocampal neurons were prepared from Sprague-Dawley rat embryos (E18). Neurons were plated at a density of $2.4x10^4$ cells/cm^2 onto 18 mm diameter cover slips pre-coated with 80 µg/ml poly-D,L-ornithine (Sigma Aldrich). Freshly dissociated cells were first plated in culture medium composed of minimum essential medium supplemented with 10% horse serum, 2 mM glutamine and 1 mM sodium pyruvate. After attachment (2-3 hours), cells were maintained in serum-free neurobasal medium supplemented with B27 and 2 mM glutamine at 37°C and 5% CO_2. For whole-cell patch-clamp recordings and epifluorescence imaging, neurons (4-10 days *in vitro*) were transiently transfected using Lipofectamine 2000 (Life Technologies) with a DNA mixture of GluN1-Y109amb-N616R or GluN1-N616R, GFP-Y182amb-GluN2B and the bidirectional plasmid pET21-tRNA-AzFRS (ratio of 1:1:1; 0.75 µg total DNA per cover slip). Immediately after transfection, AzF (1 mM) was supplied into the culture medium. Neurons were used 16-24 hours after transfection.

Two-electrode voltage clamp of *Xenopus* oocytes

For two-electrode voltage clamp recordings, the standard external solution contained (in mM): 100 NaCl, 0.3 $BaCl_2$, 5 HEPES and 2.5 KOH. The pH was adjusted to 7.3 with NaOH. NMDAR-mediated currents were induced by simultaneous application of saturating L-

glutamate and glycine at the concentrations of 100 μM each. The heavy-metal chelator diethylenetriamine-pentaacetic acid (DTPA; 10 μM) was supplemented to all bath solutions, except those for the zinc dose-response curve (DRC) experiments, to avoid inhibition by contaminant zinc (3). Unless otherwise noted, recordings were performed at a holding potential of -60 mV and at room temperature. Data were collected and analyzed using pClamp 10 (Molecular Devices) and fitted by using SigmaPlot 10.0 (SSPS) or kaleidagraph. Error bars represent the SD. of the mean value of the relative currents.

MK-801 inhibition

The MK-801 inhibition kinetics are commonly used to index relative (not absolute) P_o (9). MK-801 (Ascent Scientific) was dissolved in distilled water and prepared as 50 μM stock aliquots. MK-801 solutions were directly diluted from the stock into the full-agonist solution at the final concentration of 10 nM for GluN2A- or 50 nM for GluN2B-containing receptors. Once exposed to MK-801, the oocytes were not used for other assays. The inhibition time constants (τ_{on}) were obtained by fitting currents with a single-exponential component within a time window corresponding to 10-90% of the maximal inhibition. Each τ_{on} was normalized to the mean τ_{on} value obtained on wild-type receptors measured the same day.

Sensitivity to agonist and allosteric modulators

Glycine and glutamate DRC experiments were performed as previously described (9). Ifenprodil (generous gift from Synthélabo, France) was prepared as 10 mM stock aliquots (in 1% HCl). Zinc was prepared at 100 mM $ZnCl_2$ stock (in 1% HCl); Ifenprodil and zinc DRC were obtained and analyzed as described earlier (9).

MTS binding

MTS reagents (2-aminoethylmethanethiosulphonatehydrobromide [MTSEA], 2-(trimethylammonium)- ethylmethanethiosulphonatebromide [MTSET], 3-(triethylammonium)propylmethanethiosulphonate- bromide [MTS-PtrEA] and 2-sulfonatoethylmethanethiosulfonatesodium [MTSES]) was purchased from Toronto Research Chemicals, were dissolved in distilled water as 40 mM stock solution and stored at -20°C, and were used as previously described (5, 10). Final MTSEA (2-aminoethyl-methanethio-sulphonate-hydrobromide) solution was prepared at 200 μM concentration by immediately diluting the stock aliquots into the full-agonist solutions, and used up in less than 30 min. MTS-induced inhibition were defined as the ratio of the agonist-activated current measured after washing of the MTS divided by the current measured before MTS application. By doing so, we eliminate the contribution of the non-specific reversible channel block produced by

positively-charged MTS compounds and retain only the irreversible component of MTS-induced effects.

Redox treatment

To induce disulfide-bridge cleavage, oocytes were incubated for 15 min with DTE (dithioerythritol, 5 mM) in a Barth solution (pH 8.0) supplemented with gentamycin and D-AP5. The redox treatments on whole oocytes were performed 'offline' (on non-impaled oocytes).

Patch-clamp recordings on HEK cells and cultured neurons

Patch pipettes (5–7 MΩ) were filled with a solution containing (in mM): 115 CsF, 10 CsCl, 10 HEPES and 10 BAPTA, pH adjusted to 7.2 with CsOH. For HEK cell recordings, the external solution contained (in mM): 140 NaCl, 2.8 KCl, 1 $CaCl_2$, 10 HEPES and 0.01 DTPA, pH adjusted to 7.3 with NaOH. NMDARs were activated by applying 300 µM NMDA together with 100 µM D-serine. For recordings of cultured neurons, the external solution contained (in mM): 140 NaCl, 2.8 KCl, 1 $CaCl_2$, 10 HEPES, and 10 tricine. The agonist solution contained 300 µM NMDA, 100 µM D-serine, 1 mM $MgCl_2$ (to block endogenous NMDARs) and 300 nM free Zn^{2+} (to inhibit GluN2A-containing receptors; ref. (3)). All currents were recorded with an Axopatch 200B amplifier (Molecular Devices), sampled at 5 kHz and low-pass filtered at 2–5 kHz. The holding potential was −60 mV for HEK cells, and −80 mV for neurons. Agonists were applied using a multi-barrel rapid solution exchanger system (RSC 160, Bio-Logic).

UV exposure

For all functional recordings in *Xenopus* oocytes, online UV light treatment with PE-2 light source (CoolLED) using a 365 nm filter channeled through optical fiber was directly applied to the dark hemisphere of the oocytes in the recording chamber. Total power measured at a distance of 200 mm from the source is 105 mW (42 mW/cm^2), as reported by the manufacturer. For measurements in presence of agonists, the UV application duration was ~3 min until the UV-induced current inhibition reached a steady state. In the absence of agonist, the UV application duration was ~5 min.

UV illumination of HEK cells and cultured neurons was applied to the entire field of view using a HBO mercury light source coupled to the microscope. Light was filtered using a

DAPI dichroic mirror and projected to the sample through a 20x objective. UV was applied in the absence of agonist for 3-4 min.

Immunoblotting

Sample preparation, SDS-PAGE and immunoblotting were performed as previously described (10). The following antibodies were used: anti-GluN1 antibody (1:1,000, mouse monoclonal MAB1586 clone R1JHL; Millipore), anti-GluN2A antibody (1:500, rabbit monoclonal A12W; Millipore), anti-GluN2B antibody (1:500, mouse monoclonal 610416 clone 13; BD Transduction Laboratories), and secondary goat peroxidase-conjugated anti-mouse antibody (1:20,000, Jackson ImmunoResearch, cat. no. 115-035-003). In some cases, anti-GluN1 antibody (1:1000, mouse monoclonal MAB363 clone 54.1, Millipore) was also used as indicated in the figure legend.

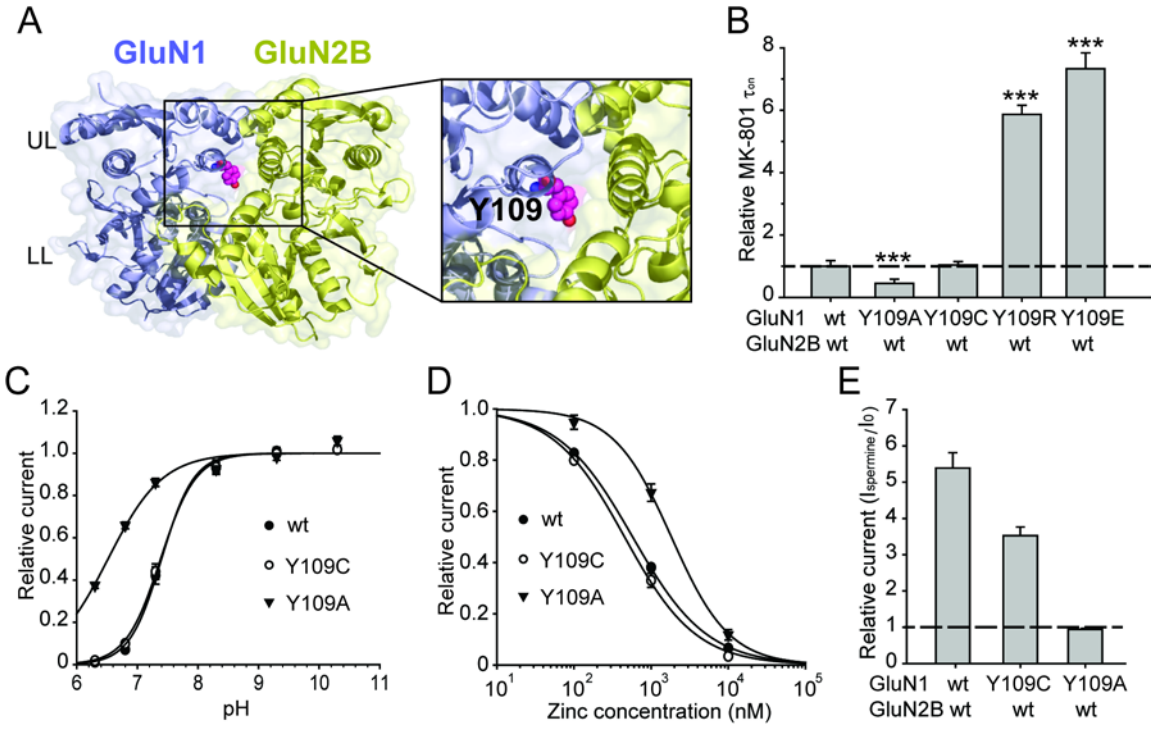

Fig. S1. GluN1-Y109 mutants alter both receptor channel activity and pharmacology.

(A) X-ray crystal structure of the GluN1/GluN2B NTD dimer (pdb code: 3QEL; ref. (11)). The GluN1 subunit is colored in light blue, and GluN2B subunit in yellow. Zoom up view of the UL/UL interface. Residue GluN1-Y109 is highlighted in purple spheres. (B) Relative inhibition kinetics by 50 nM MK-801 of receptors incorporating wild-type (wt) GluN2B subunits and GluN1 wt (1.0 ± 0.1, n=19), GluN1-Y109A (0.44 ± 0.06, n=6), GluN1-Y109C (1.04 ± 0.11, n=3), GluN1-Y109R (5.87 ± 0.29, n=3), GluN1-Y109E (7.33 ± 0.51, n=4). ***P<0.001, Student's *t*-test. (C) Proton sensitivity of GluN2B receptors containing wild-type or mutant GluN1 subunits. Values of pH_{IC50} and n_H are: 7.40 ± 0.03 and 1.6 for GluN1 wt (n=3), 7.38 ± 0.02 and 1.5 for GluN1-Y109C (n=2), 6.52 ± 0.06 and 1.0 for GluN1-Y109A (n=3). (D) Zinc dose-response curves of GluN2B receptors incorporating wild-type or mutant GluN1 subunits. IC_{50} (nM) and n_H are: 576 and 0.9 for GluN1 wt, 452 and 0.9 for GluN1-Y109C, 1829 and 1.2 for GluN1-Y109A. Maximum inhibition was fixed as 1. n=3-4 for each group. (E) 100 µM spermine potentiation of GluN2B receptors incorporating wild-type or mutant GluN1 subunits (experiments done at extracellular pH 6.6). Values of current potentiation are: 5.38 ± 0.42 for GluN1wt, 3.53 ± 0.24 for GluN1-Y109C, 0.94 ± 0.03 for GluN1-Y109A. n=3 for each group. Error bars represent the S.D.

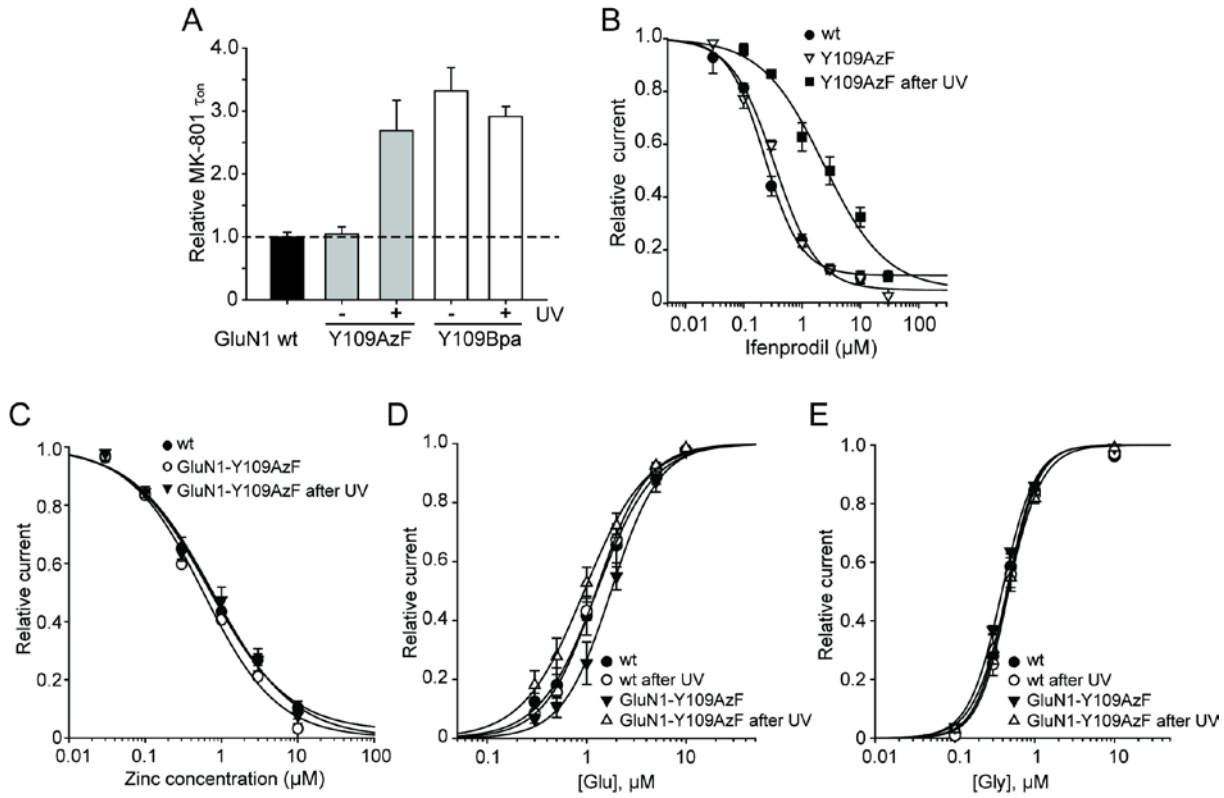

Fig. S2. Effect of UV treatment on the gating and pharmacological properties of GluN1-Y109AzF or GluN1-Y109Bpa incorporated receptors.

(A) Relative MK-801 inhibition kinetics from oocytes expressing either wt GluN1/GluN2B receptors (1.00 ± 0.07; n=7), GluN1-Y109AzF/GluN2B receptors before (1.05 ± 0.11; n=7) and after (2.69 ± 0.48; n=9) UV treatment, or GluN1-Y109Bpa/GluN2B receptors before (3.32 ± 0.37; n=6) and after (2.91 ± 0.16; n=4) UV treatment. Error bars, S.D. (B) Ifenprodil sensitivity of wt GluN1/GluN2B receptors and GluN1-Y109AzF/GluN2B receptors before and after UV treatment. IC_{50} (μM), Hill coefficients (n_H), maximal inhibition values are, respectively: 0.23 ± 0.02, 1.38, 0.90 for wt GluN1/GluN2B receptors; 0.34 ± 0.04, 1.18, 0.95 for GluN1-Y109AzF/GluN2B before UV, and 2.35 ± 0.34, 0.81, 0.95 after UV. n=3-4 for each group. (C) Zinc dose-response curves for wt GluN1/GluN2B receptors (IC_{50} = 0.68 μM, n_H = 0.83, and $Inhibition_{max}$ = 0.98), GluN1-Y109AzF/GluN2B wt receptors before (IC_{50} = 0.58 μM, n_H = 0.89, and $Inhibition_{max}$ = 1.00) and after (IC_{50} = 0.77 μM, n_H = 0.82, and $Inhibition_{max}$ = 0.98) UV treatment. n=3-4 for each group. (D) Glutamate dose-response curves for wt GluN1/GluN2B receptors before (EC_{50} =1.27 μM, n_H =1.52) and after UV (EC_{50} = 1.24 μM, n_H = 1.69); for GluN1-Y109AzF/GluN2B wt receptors before (EC_{50} = 1.77 μM, n_H = 1.78) and after (EC_{50} = 0.96 μM, n_H = 1.40) UV treatment. n=3 for each group. (E) Glycine dose-response curves for wt GluN1/GluN2B receptors before (EC_{50} = 0.44 μM, n_H = 2.3) and after UV (EC_{50} = 0.47 μM, n_H = 2.3); for the GluN1-Y109AzF/GluN2B wt receptors before (EC_{50} = 0.39 μM, n_H = 2.1) and after (EC_{50} = 0.46 μM, n_H = 2.00) UV treatment. n = 3-4 for each group. Error bars, S.D.

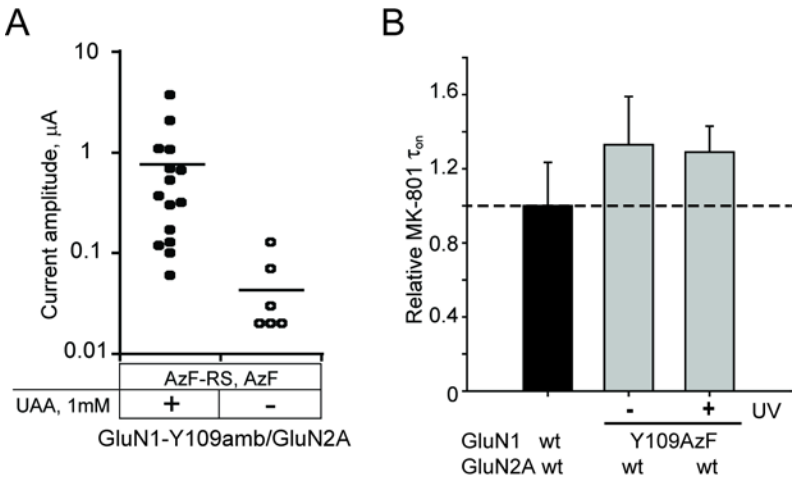

Fig. S3. Genetically encoding AzF in GluN1/GluN2A receptors

(A) Representative dot plot of the current amplitudes from oocytes injected with plasmids encoding GluN1-Y109amb (40 ng/µl), GluN2A-wt (40 ng/µl), Yam suppressor tRNA (5 ng/µl), and AzF-RS (1ng/µl) in the absence (empty circles) or presence (solid circles) of the UAA in the incubation media. For each condition, 20 oocytes were tested. Only currents >10 nA were plotted. (B) Relative inhibition kinetics by 10 nM MK-801 applied to oocytes expressing wild-type (wt) GluN1/GluN2A receptors (1.00 ± 0.24), GluN1-Y109AzF/GluN2A before (1.33 ± 0.26) and after (1.29 ± 0.14) UV treatment. n=3 for each group. Error bars represent the S.D.

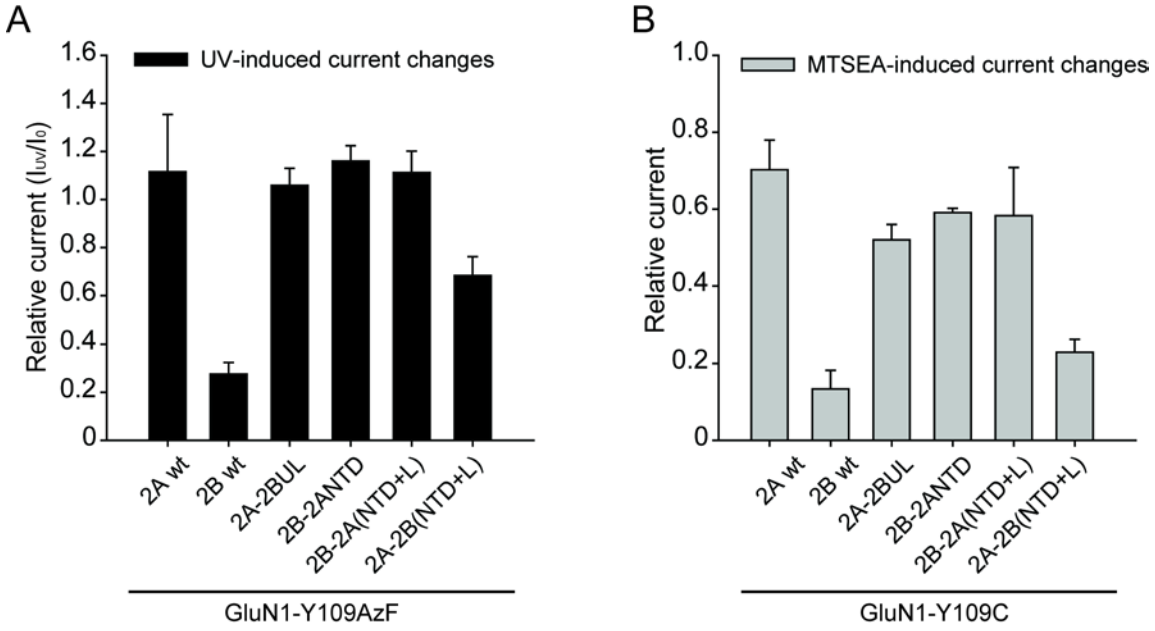

Fig. S4. Modulating UV- and chemical-induced receptor alterations by GluN2A and GluN2B NTD chimeras

(A) UV modification of current carried by receptors containing GluN1-Y109AzF subunits and GluN2A wt (1.12 ± 0.24), GluN2B (0.28 ± 0.05), GluN2A-2BUL (1.06 ± 0.07), GluN2B-2ANTD (1.16 ± 0.06), GluN2B-2A(NTD+L) (1.11 ± 0.09) or GluN2A-2B(NTD+L) (0.68 ± 0.08). n=3-16 for each group. (B) MTSEA modification at GluN1-Y109C receptors containing various GluN2 subunits. Values are: GluN2A wt (0.70 ± 0.08), GluN2B wt (0.13 ± 0.05), GluN2A-2BUL (0.52 ± 0.04), GluN2B-2ANTD (0.59 ± 0.01), GluN2B-2A(NTD+L) (0.58 ± 0.13), GluN2A-2B(NTD+L) (0.23 ± 0.03). n = 3-12 for each group. Error bars represent the S.D.

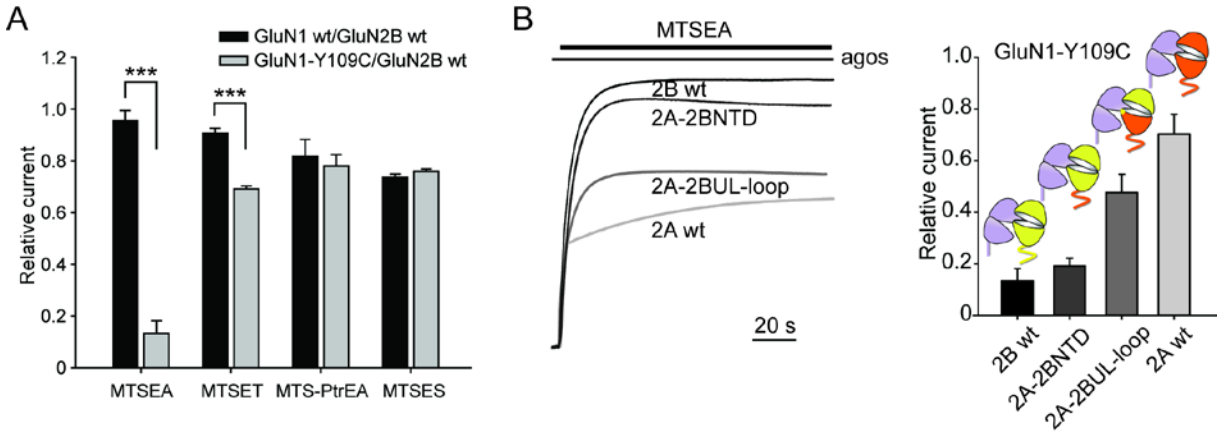

Fig. S5. Subunit specific changes in receptor activity induced by MTSEA binding to the GluN1-Y109C mutant.

(A) MTS reagent current modifications at GluN2B receptors containing either wild-type (wt) GluN1 or GluN1-Y109C mutant subunits. Values from left to right are: 0.95 ± 0.04, 0.13 ± 0.05 for MTSEA; 0.91 ± 0.02, 0.69 ± 0.01 for MTSET; 0.82 ± 0.07, 0.78 ± 0.04 for MTS-PtrEA, 0.74 ± 0.01, 0.76 ± 0.01 for MTSES. n=3-8 for each group. (B) Left panel: UV modification of current carried by receptors containing GluN1-Y109AzF subunits and GluN2A wt (1.12 ± 0.24), GluN2B (0.28 ± 0.05), GluN2A-2BUL (1.06 ± 0.07), GluN2B-2ANTD (1.16 ± 0.06), GluN2B-2A(NTD+L) (1.11 ± 0.09) or GluN2A-2B(NTD+L) (0.68 ± 0.08). n=3-16 for each group. Right panel: MTSEA modification at GluN1-Y109C receptors containing various GluN2 subunits. Values are: GluN2A wt (0.70 ± 0.08), GluN2B wt (0.13 ± 0.05), GluN2A-2BUL (0.52 ± 0.04), GluN2B-2ANTD (0.59 ± 0.01), GluN2B-2A(NTD+L) (0.58 ± 0.13), GluN2A-2B(NTD+L) (0.23 ± 0.03). n = 3-12 for each group. Error bars represent the S.D. ***P<0.001, Student's *t*-test. Only the MTS-specific irreversible component of the inhibitory effects on receptor activity is taken into account for the calculation of relative currents (see SI Material and Methods).

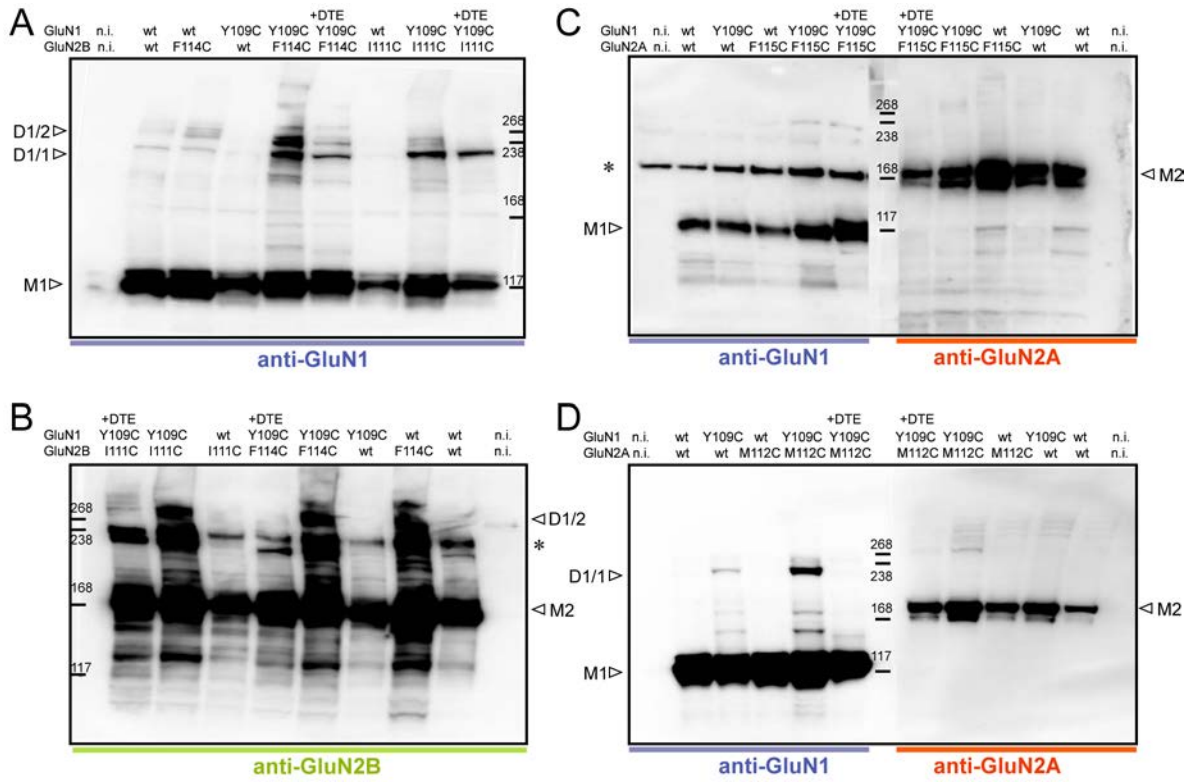

Fig. S6. Differential NTD UL/UL interface in GluN2A- and GluN2B- containing receptors.

(A,B) Immunoblots from *Xenopus* oocytes expressing either wt or mutant GluN1 and GluN2B subunits detected by anti-GluN1 (blue) or anti-GluN2B (yellow) antibodies. M1 indicates the expected band location of the GluN1 monomer (~110 kDa); M2 indicates the expected band location of the GluN2B monomer (~180 kDa); D1/2 indicates the expected band location of the GluN1/GluN2B heterodimer (~290 kDa); D1/1 indicates the expected band location of the GluN1 homodimer (~220 kDa). * indicates a non-specific band. n.i. indicates non-injected oocytes. Treatment with the reducing reagent DTE is also marked (+DTE). (C,D) Immunoblots from *Xenopus* oocytes expressing either wild-type (wt) or mutant GluN1 and wt or mutant GluN2A subunits detected by anti-GluN1 (blue) or anti-GluN2A (orange) antibodies. M1 indicates the expected band location of the GluN1 monomer (~110 kDa); M2 indicates the expected band location of the GluN2A monomer (~180 kDa); D1/1 indicates the expected band location of the GluN1 homodimer (~220 kDa). The anti-GluN1 antibodies MAB363 and MAB1586 were used in (A,C) and (D), respectively.

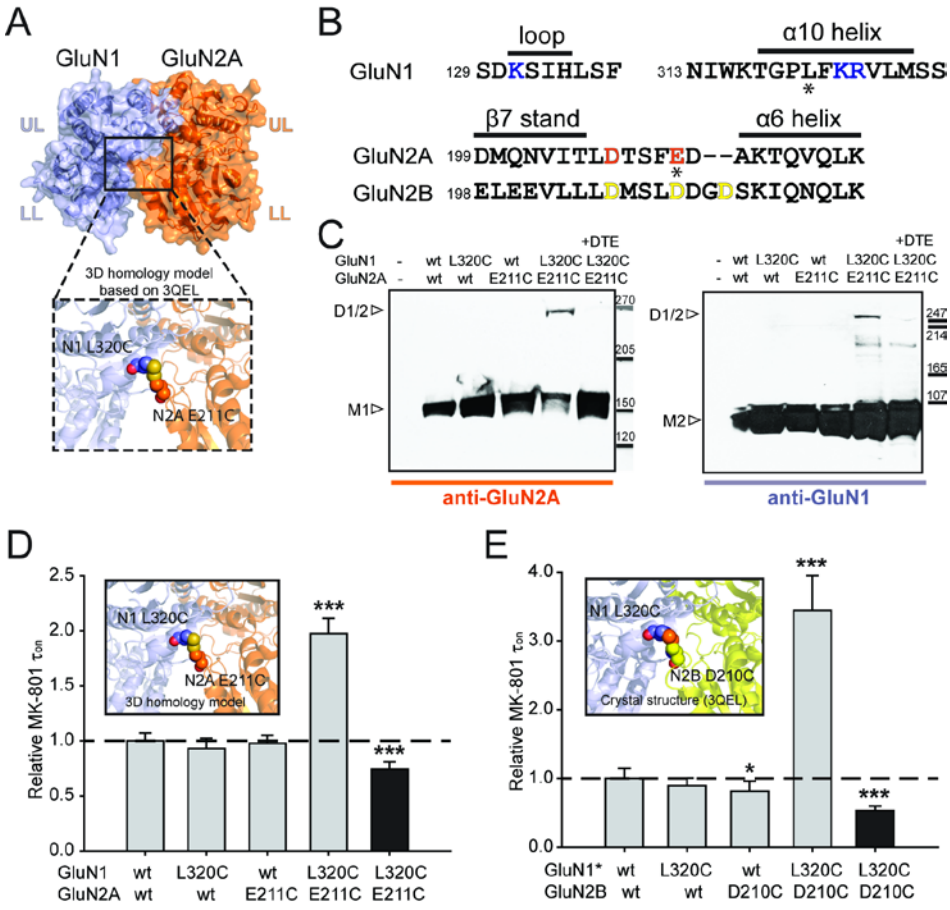

Fig. S7. Engineering a disulfide bond at the GluN1 UL/GluN2 LL NTD dimer interface affects receptor activity.

(A) 3D homology model of the GluN1/GluN2A NTD heterodimer based on GluN1/GluN2B NTD crystal structure (pdb code: 3QEL; ref. (11)). The putative interface formed by the GluN1 NTD upper lobe (UL) and the GluN2A NTD lower lobe (LL) is boxed. Inset: sphere representation of the residues mutated into cysteines: GluN1-L320 (purple) and GluN2A-E211 (orange). (B) Sequence alignment in the region around the GluN1 UL/GluN2 LL interface. Residues mutated into cysteines are indicated with asterisks (GluN1-L320 and GluN2A-E211). The residues contributing to the electrostatic interactions are colored in purple for GluN1 (K131, K322 and R323), orange for GluN2A (D207 and E211) and yellow for GluN2B (D206, D210 and D213), respectively. (C) Immunoblots from *Xenopus* oocytes expressing GluN1/GluN2A receptors incorporating either wild-type (wt) or cysteine mutant subunits. The GluN1 monomer band (M1) is ~110 kDa, while the GluN2A monomer band (M2) is ~180 kDa. The D1/2 arrowheads indicate the GluN1/GluN2A disulfide-linked heterodimer (absent in DTE). (D) Relative MK801 inhibition kinetics of GluN1/GluN2A receptors incorporating wt or cysteine mutant subunits. Inset: Close-up view of the modelled GluN1 UL/GluN2A LL NTD dimer interface. Mean values are, from left to right: 1.00 ± 0.06 (n=9), 0.93 ± 0.09 (n=6), 0.98 ± 0.07 (n=6), and the double-cysteine receptors before, 1.98 ± 0.14 (n=9), and after (black bar), 0.74 ± 0.07 (n=6), DTE treatment. (E) Relative MK801 inhibition kinetics of GluN1/GluN2B receptors incorporating wt or cysteine mutant subunits. GluN1* represents the GluN1-C744A-C798A mutant subunit (9, 12). Inset: Close-up view of the GluN1 UL/GluN2B LL NTD dimer interface as seen in the GluN1/GluN2B NTD dimer crystal structure (11). The two introduced cysteines, GluN1-L320C and GluN2B-D210C are indicated in sphere. Mean values are, from left to right: 1.00 ± 0.12 (n=9), 0.89 ± 0.11 (n=7), 0.81 ± 0.15 (n=10), and the double cysteine containing receptors before, 3.45 ± 0.50 (n=6), and after (black bar), 0.53 ± 0.06 (n=5), DTE treatment. *P<0.05, ***P<0.001, Student's *t*-test. Error bars represent the S.D.

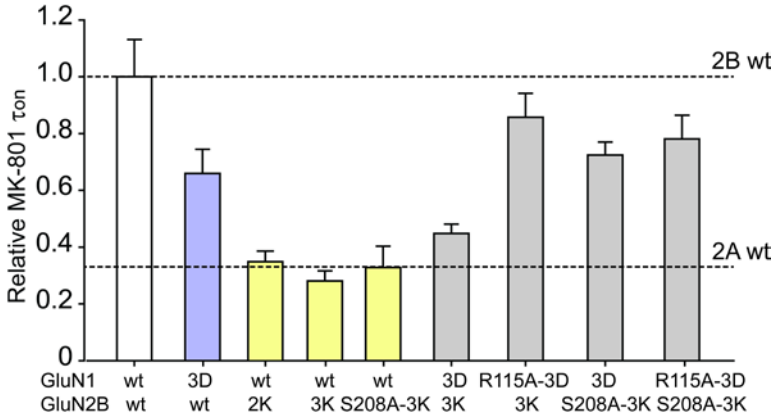

Fig. S8. Electrostatic interactions at the GluN1-UL/GluN2B-LL NTD dimer interface.

Relative MK-801 inhibition kinetics of receptors incorporating wild-type (wt) or mutant GluN1, and wt or mutant GluN2B subunits. Values from left to right are: GluN1 wt/GluN2B wt (1.00 ± 0.13; n=35), GluN1-3D/GluN2B wt (0.66 ± 0.09; n=8), GluN1wt/GluN2B-2K (referring to D206K-D210K; 0.35 ± 0.04; n=8), GluN1 wt/GluN2B-3K (0.28 ± 0.04; n=9), GluN1 wt/GluN2B-S208A-3K (0.33 ± 0.07; n=6), GluN1-3D/GluN2B-3K (0.45 ± 0.03; n=4), GluN1-R115A-3D/GluN2B-3K (0.85 ± 0.08; n=8), GluN1-3D/GluN2B-S208A-3K (0.72 ± 0.05; n=2), GluN1-R115A-3D/GluN2B-S208A-3K (0.78 ± 0.08; n=6). Error bars represent the S.D.

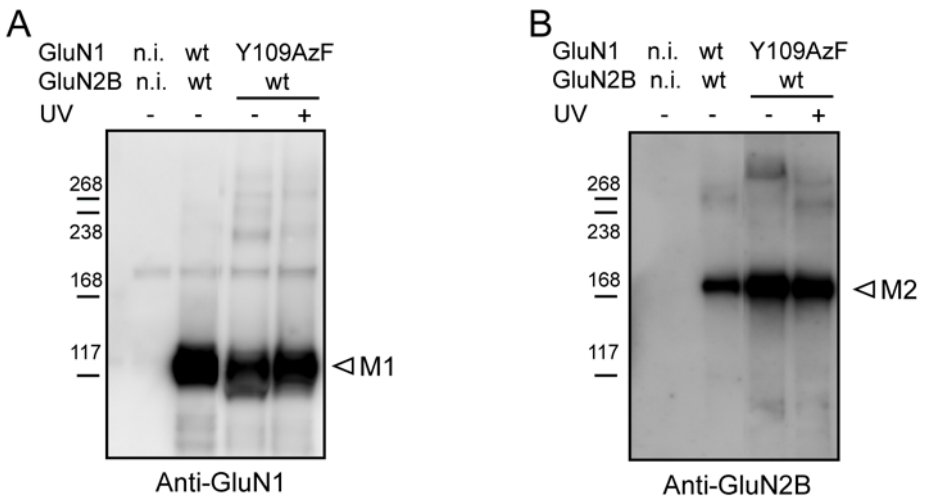

Fig. S9. No heterodimer formation after UV-treatment of GluN1-Y109AzF/GluN2B receptors.

Western blots from *Xenopus* oocytes expressing wild-type (wt) GluN1/GluN2B or GluN1-Y109AzF/GluN2B receptors probed either with anti-GluN1 (left) or anti-GluN2B (right) antibodies. GluN1 monomers (M1, ~110 kDa) or GluN2B monomers (M2, ~180 kDa) are indicated with arrowheads. The - and + signs refer to the absence or presence, respectively, of UV irradiation (365 nm, 30 min). n.i. indicates non-injected oocytes.

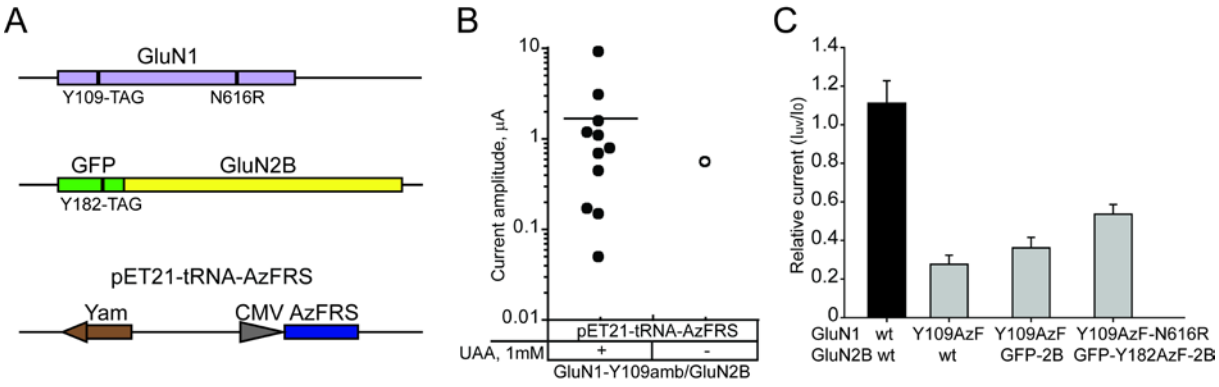

Fig. S10. Optimization and validation in *Xenopus* oocytes of molecular biology constructs for expression of AzF containing NMDARs in mammalian cells

(A) Plasmid constructions designed for mammalian cell transfections. One plasmid encodes the GluN1 subunit with the Y109 site mutated to the amber stop codon and the N616 at the Q/R/N pore site mutated to R in order to confer resistance to extracellular Mg^{2+} block. Another plasmid encodes the GFP fused to the N-terminal of the GluN2B subunit. The amber stop codon was inserted at the Y182 position of the GPF, in order to use green GFP fluorescence as a reporter of AzF incorporation. One bidirectional plasmid named pET21-tRNA-AzFRS encodes the suppressor tRNA Yam driven by its internal promoter and the AzFRS driven by the CMV promoter. (B) Current amplitudes from oocytes co-injected with GluN1-Y109amb, wild-type (wt) GluN2B and pET21-tRNA-AzFRS plasmids, incubated in the absence (n=9) or presence (n=15) of the UAA AzF. Only currents >10 nA were plotted. (C) UV-induced current modifications at GluN1 wt/GluN2B wt (1.11 ± 0.13; n=8), GluN1-Y109AzF/GluN2B wt (0.28 ± 0.05; n=16), GluN1-Y109AzF/GFP-GluN2B (0.31 ± 0.03; n=5), and GluN1-Y109AzF-N616R/GFP-Y182AzF-GluN2B receptors (0.54 ± 0.05; n=5). Error bars represent the S.D.

References

1. Ye S*, et al.* (2008) Site-specific incorporation of keto amino acids into functional G protein-coupled receptors using unnatural amino acid mutagenesis. *The Journal of biological chemistry* 283(3):1525-1533.
2. Ye S, Huber T, Vogel R, & Sakmar TP (2009) FTIR analysis of GPCR activation using azido probes. *Nat Chem Biol* 5(6):397-399.
3. Paoletti P, Ascher P, & Neyton J (1997) High-affinity zinc inhibition of NMDA NR1-NR2A receptors. *J Neurosci* 17(15):5711-5725.
4. Gielen M*, et al.* (2008) Structural rearrangements of NR1/NR2A NMDA receptors during allosteric inhibition. *Neuron* 57(1):80-93.
5. Gielen M, Siegler Retchless B, Mony L, Johnson JW, & Paoletti P (2009) Mechanism of differential control of NMDA receptor activity by NR2 subunits. *Nature* 459(7247):703-707.
6. Kang JY*, et al.* (2013) In vivo expression of a light-activatable potassium channel using unnatural amino acids. *Neuron* 80(2):358-370.
7. Luo JH*, et al.* (2002) Functional expression of distinct NMDA channel subunits tagged with green fluorescent protein in hippocampal neurons in culture. *Neuropharmacology* 42(3):306-318.
8. Ye S, Riou M, Carvalho S, & Paoletti P (2013) Expanding the genetic code in Xenopus laevis oocytes. *Chembiochem* 14(2):230-235.
9. Zhu S, Stroebel D, Yao CA, Taly A, & Paoletti P (2013) Allosteric signaling and dynamics of the clamshell-like NMDA receptor GluN1 N-terminal domain. *Nat Struct Mol Biol* 20(4):477-485.
10. Mony L, Zhu S, Carvalho S, & Paoletti P (2011) Molecular basis of positive allosteric modulation of GluN2B NMDA receptors by polyamines. *EMBO J* 30(15):3134-3146.
11. Karakas E, Simorowski N, & Furukawa H (2011) Subunit arrangement and phenylethanolamine binding in GluN1/GluN2B NMDA receptors. *Nature* 475(7355):249-253.
12. Sullivan JM*, et al.* (1994) Identification of two cysteine residues that are required for redox modulation of the NMDA subtype of glutamate receptor. *Neuron* 13(4):929-936.